Friction **11**(4): 538–545 (2023)
https://doi.org/10.1007/s40544-022-0613-x
ISSN 2223-7690
CN 10-1237/TH
RESEARCH ARTICLE

Intermittent failure mechanism and stabilization of microscale electrical contact

Tianbao MA[1,†,*], Zhiwei YU[1,2,†], Aisheng SONG[1], Jiahao ZHAO[3,4,5], Haibo ZHANG[6], Hongliang LU[7,8], Dandan HAN[3,4,5], Xueyan WANG[7,8], Wenzhong WANG[6]

[1] *State Key Laboratory of Tribology, Tsinghua University, Beijing 100084, China*
[2] *Inspur Beijing Electronic Information Industry Co., Ltd., Beijing 100085, China*
[3] *Department of Precision Instrument, Tsinghua University, Beijing 100084, China*
[4] *Innovation Center for Future Chips, Beijing 100084, China*
[5] *State Key Laboratory of Precision Measurement Technology and Instruments, Beijing 100084, China*
[6] *School of Mechanical Engineering, Beijing Institute of Technology, Beijing 100081, China*
[7] *School of Physical Sciences, University of Chinese Academy of Sciences, Beijing 100049, China*
[8] *Institute of Physics, Chinese Academy of Sciences, Beijing 100190, China*

Received: 10 February 2022 / Revised: 21 February 2022 / Accepted: 28 February 2022

Abstract: The stability and lifetime of electrical contact pose a major challenge to the performance of micro-electro-mechanical systems (MEMS), such as MEMS switches. The microscopic failure mechanism of electrical contact still remains largely unclear. Here conductive atomic force microscopy with hot switching mode was adopted to simulate the asperity-level contact condition in a MEMS switch. Strong variation and fluctuation of current and adhesion force were observed during 10,000 repetitive cycles, exhibiting an "intermittent failure" characteristic. This fluctuation of electrical contact properties was attributed to insulative carbonaceous contaminants repetitively formed and removed at the contact spot, corresponding to degradation and reestablishment of electrical contact. When contaminant film was formed, the contact interface became "metal/carbonaceous adsorbates/metal" instead of direct metal/metal contact, leading to degradation of the electrical contact state. Furthermore, a system of iridium/graphene on ruthenium (Ir/GrRu) was proposed to avoid direct metal/metal contact, which stabilized the current fluctuation and decreased interfacial adhesion significantly. The existence of graphene enabled less adsorption of carbonaceous contaminants in ambient air and enhanced mechanical protection against the repetitive hot switching actions. This work opens an avenue for design and fabrication of microscale electrical contact system, especially by utilizing two-dimensional materials.

Keywords: atomic force microscopy; microscale electrical contact; graphene

1 Introduction

The performance and reliability of micro/nano-scale electrical contacts are key issues for research in the field of micro/nano devices, especially in the field of micro-electro-mechanical system (MEMS) switches [1]. Although traditional noble metal contact materials show excellent electrical conductivity and high chemical inertness, they still face the problem of contact failure caused by unstable contact resistance and permanent adhesion with increasing demands for a long lifetime [2–5]. The major causes of the

† Tianbao MA and Zhiwei YU contributed equally to this work.
* Corresponding author: Tianbao MA, E-mail: mtb@mail.tsinghua.edu.cn

contact resistance failure include native metal oxidation and adsorbate/tribopolymer formation on the contact surfaces [2–4, 6]. On the other hand, materials transfer, chemical bonds formation, or adhesive wear may result in adhesive failure and even permanent closure of switches [5].

Recently, two-dimensional (2D) materials, such as graphene and MoS_2, have arouse great interests in the field of electrical contacts due to their low surface energy, excellent mechanical, electrical, and tribological properties [7–9]. However, 2D materials face the challenge of high interfacial contact resistance across van der Waals gaps [10, 11]. Despite great efforts on micro/nano-scale electrical contacts in past decades, how to design suitable contact materials and how to achieve a stable and long-lasting electrical contact state with low contact resistance and low adhesion performance still remain challenges. In this paper, we have studied the performance and failure mechanisms of asperity-level electrical contacts in metal/metal, metal/graphene system by using conductive atomic force microscope (C-AFM), and proposed a novel architecture by introducing graphene at the interface to stabilize electrical contact properties.

C-AFM has been recently adopted as a powerful tool to measure interfacial contact resistance and to screen potential electrical contact materials [2, 12–17]. A representative work was performed by Streller et al. using C-AFM to mimick the contact conditions in nanoelectromechanical (NEM) contact switches, which showed 10,000 times increase in contact resistance and 12% increase in adhesion force after 1.5 billion tip-tapping cycles [2]. It is generally accepted that sharp AFM tips can form single-asperity contact geometry with flat samples. However, in MEMS switches, the size of the contact is in micrometer scale, thus the real contact is a collection of single-asperity contacts. So we firstly tested if the AFM contact geometry can qualitatively simulate the asperity-level contact condition in a MEMS switch, i.e., whether the contact pressure and current density are equivalent between the two situations.

2 Results and discussion

The commercial MEMS switch chosen to be analyzed here was purchased from Analog Devices, Inc. The upper electrode (cantilever beam) of the switch was cut by focused ion beam (FIB) and transferred to a copper foil, where the contact of the upper electrode showed a spherical shape with a diameter of 2–2.5 μm (indicated by the red arrow in Fig. 1(a)). Cross-sectional tunneling electron microscopy (TEM) of the upper contact showed a Ru coating with a thickness of 100 nm on Au substrate (Fig. 1(b)). The contact of the lower electrode was also coated with Ru coating. In order to analyze the contact condition of the switch, the surface morphologies of the upper and lower contact were firstly measured respectively by AFM contact mode as shown in Figs. 1(c) and 1(d). Then numerical simulations were conducted to calculate the contact pressure distribution (Fig. 1(e)), where the Young's modulus and Possion's ratio for Ru are 447 GPa and 0.3, respectively. Under a normal load of 50 μN, only three separate contact regions were formed between the upper and the lower Ru surfaces due to surface roughness (Fig. 1(f)). The local contact pressure was 15.7 GPa and the real contact area was summed to be 3,173.8 nm^2. Since the drain source current is 50 mA for the switch which is the sum current passing through 5 switches in parallel connection. Thus the current density passing through the calculated real contact region here was estimated to be 3.2 $\mu A/nm^2$. This contact situation could be approximately realized in a single-asperity contact between AFM Ir tip with a radius of curvature of 10 nm and Ru surface, under a normal load of 100 nN, and with a circuit current of about 10 μA (Young's modulus and Possion's ratio for Ir are 528 GPa and 0.26, respectively), where the contact pressure and current density were estimated to be 15.8 GPa and 1.6 $\mu A/nm^2$, respectively. Hence if not mentioned explicitly here, Ir tip with a radius of curvature of about 10 nm and applied load of 100 nN was adopted in following tests in order to qualitatively simulate the asperity-level contact condition in MEMS switch.

The C-AFM experimental setup of asperity-level electrical contact measurement is shown in Fig. 2(a) (Cypher AFM, Oxford Instruments). An Ir coated AFM tip (ASYELEC.01-R2, tip radius R = 12 nm, force constant k = 3.81 $N \cdot m^{-1}$) was used. The test was conducted in ambient atmosphere under temperature

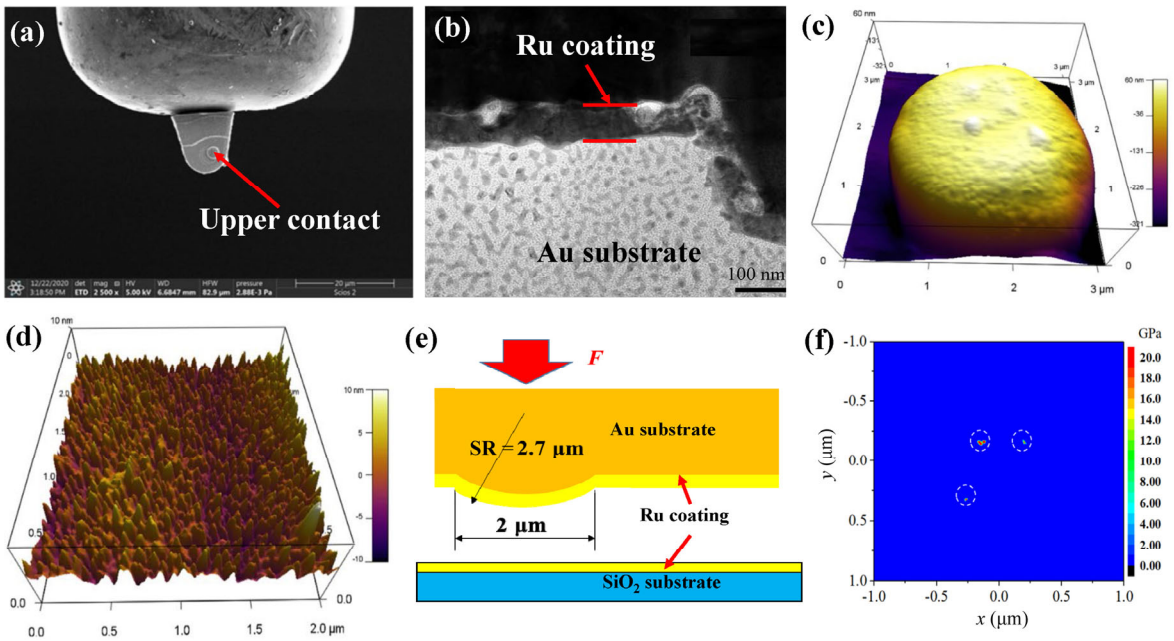

Fig. 1 Characterization of commercial MEMS switch and analysis of multi-asperity contact condition. (a) Scanning electron microscopy (SEM) image of the upper contact of MEMS switch cut and transferred by FIB; (b) cross sectional TEM view of the upper contact showing the Ru coating with a thickness of about 100 nm; (c) morphology measurement of the upper contact; (d) morphology measurement of the lower contact; (e) multi-asperity contact mechanics model; and (f) numerical calculation of contact pressure distribution under 50 μN load.

of 25 °C and relative humidity of 45%. The conductive tip was driven to repetitively "approach–retract" a conductive sample (including Au coated Si, Ru coating on Au coated Si, and graphene on Ru substrate in this work). Hot switching mode was adopted by applying a bias voltage (90 mV) between tip and sample during the "approach–retract" cycles (each cycle with a duration of 1 s). In each cycle, the normal force curve (normal force vs. displacement) and current curve (current vs. displacement) were obtained simultaneously, as shown in Fig. 2(b). In order to study the time evolution of electrical contact behavior during a long duration as shown in Fig. 2(c), we recorded the instant current when maximum load of 100 nN was achieved during each approaching process, and the adhesion force obtained in each "approach–retract" cycle.

Strong fluctuation of current and adhesion force can be observed during 10,000 cycles, exhibiting an "intermittent failure" characteristic. It was found that the current sometimes leveled off at around 8.5 μA (corresponding to a contact resistance around 0.6 kΩ, calculated considering the 10 kΩ protection resistance connected in series with the sample as denoted in Fig. 2(a)). Interestingly, the current sometimes dropped significantly, but resumed to the level-off state after a while. And adhesion force sometimes leveled off at around 5 nN, but increased after a while to values in a range of several tens to 100 nN. Most probable reasons for this "intermittent failure" phenomenon could be worn-out of the conducting metal coating, or formation of non-conducting contaminants at the contact. Here the nominal thickness of Ir coating on AFM tip was about 20 nm. We compared the tip morphology by High-resolution tunneling electron microscopy (HRTEM) before and after the hot switching electrical contact test (Figs. 2(d) and 2(e)), and found no visible wear (less than 1 nm). So the "worn-out" postulation could be generally excluded. Instead, some additional substances were found on the tip apex with a thickness of about 2 nm. XPS characterization of the sample of Au coating (Fig. 2(f)) showed evidence of carbonaceous adsorbates which may originate from contaminants in ambient air, which was in consistence with previous studies [2, 3, 6].

In order to unravel the intermittent failure mechanism, we focused on the evolution of electrical contact properties during a period of time with intermittent failure (450–650 cycles shown in Fig. 3(a)).

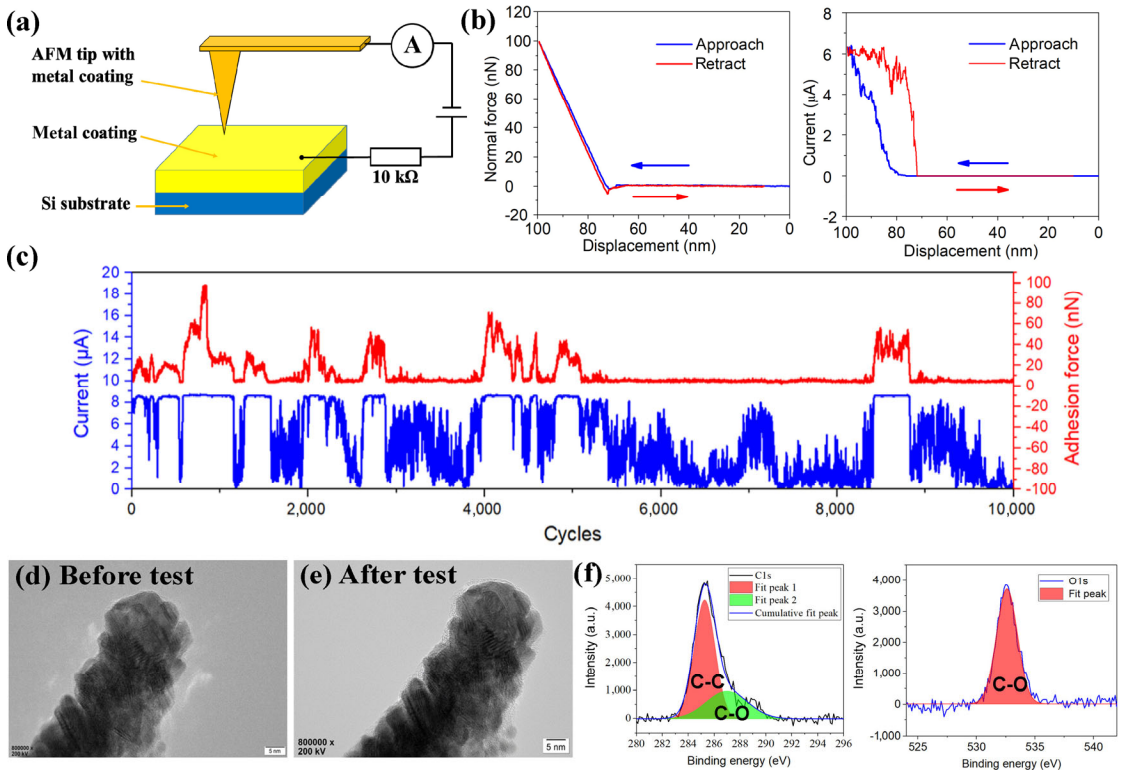

Fig. 2 Schematic of hot switching test, results, and characterization. (a) C-AFM experiment setup. Three samples were used in this work: Si substrate with 100 nm-thick Au coating, 100 nm-thick Ru coating on Au coated Si, and monolayer graphene on Ru substrate; (b) normal force curve and current curve obtained simultaneously during a typical "approach–retract" process; (c) variation of current and adhesion force during 10,000 repetitive cycles; (d, e) HRTEM images of AFM tip apex before and after hot switching test; and (f) X-ray photoelectron spectroscopy (XPS) characterizations of Au coating showing existence of carbonaceous adsorbates.

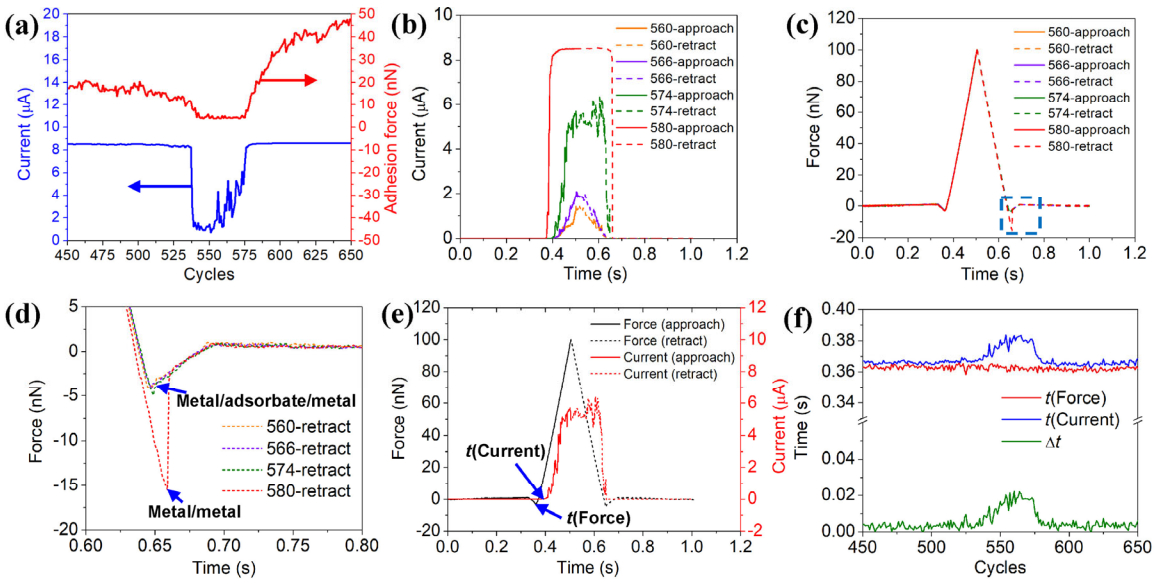

Fig. 3 Detailed analysis of intermittent failure. (a) Enlargement of Fig. 2(c) during 450─650 cycles; (b) current curves during the entire approach─retract processes of 560, 566, 574, and 580 cycles, solid lines represented approach process and dashed lines represented retract process; (c) force curves during the entire approach–retract processes of 560, 566, 574, and 580 cycles; (d) enlargement of rectangle in Fig. 3(c) emphasizing the pull-out stages; (e) definition of time of mechanical contact (t(Force)), and time of electrical contact (t(Current)) from the force and current curve during 574th cycle; and (f) evolution of retardation time ($\Delta t = t$(Current) – t(Force)) during 450–650 cycles.

From 450 to 537 cycles, it remained stable at "high current" stage. At 538th cycle, the current dropped from the high value abruptly to as low as 1 μA (corresponding to contact resistance of about 80 kΩ), suggesting degradation of electrical contact, meanwhile, the adhesion force decreased to a level-off value of about 5 nN. Then the current fluctuated and gradually increased, suggesting reestablishment of electrical contact. After about 580th cycle, the current resumed to the high value, and the adhesion force significantly increased from the level-off state. This variation and fluctuation in current curve suggested complex degradation and reestablishment processes of the electrical contact state between tip and sample. Together with the above characterizations, we speculated that this is due to the insulative contaminants repetitively formed and removed at the contact spot. That is to say, when contaminant film was formed, the contact interface actually becomes "metal/carbonaceous adsorbate/metal" instead of direct metal/metal contact, leading to degradation of the electrical contact state. When contaminant film was removed or penetrated by the repetitive tip contact action, effective electrical contact between the tip and sample will be reestablished. Furthermore, the dynamic process in a single "approach–retract" cycle was carefully analyzed as shown in Figs. 3(b) and 3(c). It is observed clearly that the electrical contact behavior changed much from 560 to 580 cycles. During the approach process of 560th cycle, the current increased slowly to a relatively low value, indicating a "metal/insulative adsorbate/metal" contact. With increasing cycles, the slope of current–time curves increased obviously, the current increased very fast to the high value during the approach process of the 580th cycle, indicating reestablishment of "metal/metal" electrical contact. By comparison of the force curves at the pull-off stage (Fig. 3(d), an enlargement of the rectangle in Fig. 3(c)), it was observed that the adhesion force for "metal/metal" contact was considerably larger than that for "metal/insulative adsorbate/metal" contact. It should also be mentioned that high current was always accompanied by large adhesion force and low adhesion force generally existed during the intermittent electrical contact failure. This again demonstrates the dilemma faced in this research area that high electrical contact conductance and low friction/wear/adhesion cannot be perfectly satisfied simultaneously.

Another evidence for the existence of insulative contaminant film was the retardation of electrical contact with regard to mechanical contact as shown in Figs. 3(e) and 3(f). The retardation time was defined as the time corresponding to the lowest point (pull-in to contact) of force curve (t(Force)), subtracted by the time when current started increasing from zero (t(Current)) as shown in Fig. 3(e). Obvious retardation of electrical contact can be observed during the intermittent failure process, i.e., electrical contact was established later after mechanical contact (Fig. 3(f)). This suggested that although the tip and sample (actually, thin adsorbate layer on sample) was already "physically" in contact, electrical contact was not established until the tip further indented the adsorbate layer. It is known that electron tunneling plays a major role in transmitting current when very thin insulating film exists at the electrical contact interface [18, 19]. So the existence of the adsorbate contaminant film resulted in degradation of the electrical contact performance.

As discussed above, it is challenging to achieve high electrical contact conductance and low adhesion simultaneously. In some high-precision signal transmission situation where the stability and lifetime of electrical contact is the major concern, it will require less fluctuation of the electrical signal, while the absolute magnitude of current is not the main focus. Here we show that a novel architecture of iridium/graphene on ruthenium (Ir/GrRu) could achieve low adhesion and stable electrical contact. The experimental setup and procedure were quite similar to that shown in Fig. 2(a), the Ir coated conductive tip was used, and a normal load of 400 nN was applied. The relative humidity was 12%. Graphene grown on Ru substrate was used as the sample. The sample was prepared by chemical vapor deposition (CVD) method. The Ru (0001) substrate was exposed to ethylene with partial pressure 1.4×10^{-4} Pa at 850 °C for 100 s and graphene was formed by the thermal decomposition of ethylene. More details could be found in previous work [20]. In order to illustrate the advantages of the Ir/GrRu system, electrical contact between Ir and 100 nm-thick Ru coating on Au coated Si (Ir/Ru) was also tested as a reference system.

As shown in Figs. 4(a) and 4(b), Ir/GrRu system

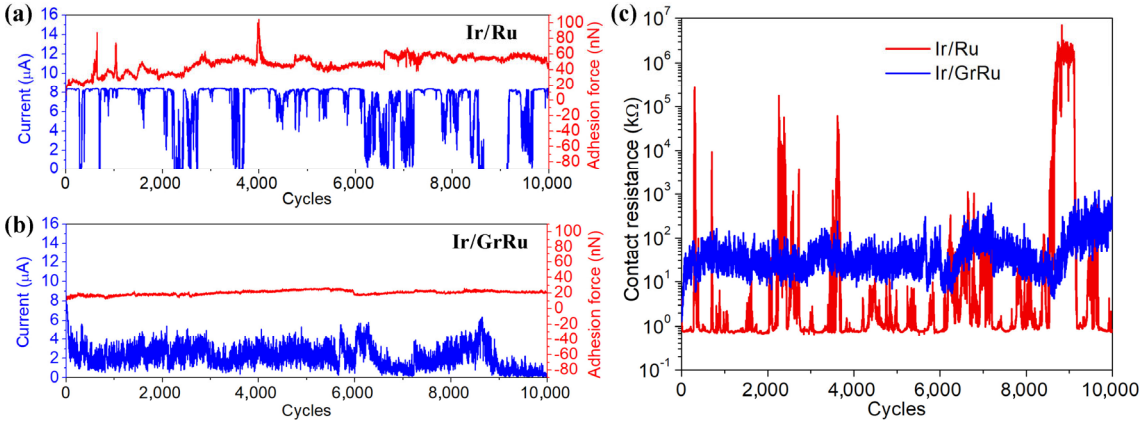

Fig. 4 Comparison of Ir/Ru and Ir/GrRu electrical contact system. The Ir-coated tip was used with a normal load of 400 nN. (a, b) Variation of current and adhesion force during 10,000 repetitive cycles for Ir/Ru system and Ir/GrRu system; and (c) comparison of the contact resistance between two systems.

exhibited much lower and stable adhesion force than Ir/Ru system during 10,000 repetitive hot switching cycles. The current curve of Ir/Ru system showed high current level-off stages, which has been proved to be a result of direct metal/metal contact in the above section. However, intermittent failure was observed. In contrast, Ir/GrRu system showed generally lower current with time evolution, however, it remained relatively stable without vanishing current. As shown in Fig. 4(c), although the absolute value of contact resistance of Ir/GrRu was about one order of magnitude higher than the high current stage of Ir/Ru, the contact resistance remained quite stable during the 10,000 repetitive hot switching cycles, and showed no intermittent failure. In Ir/Ru system, however, the contact resistance can increase to even 5–6 orders of magnitude higher due to the degradation of the electrical contact. The results showed both the advantages and disadvantages of graphene as electrical contact material. The introduction of graphene at the interface could avoid direct metal/metal contact and hence decreased interfacial adhesion significantly. Also graphene is chemically less active than metal and has much lower surface energy, resulting in less adsorption of carbonaceous contaminants in ambient air. So it is relatively "clean" and mechanically protective during the repetitive hot switching cycles. Unfortunately, graphene will introduce van der Waals gap and additional tunneling barrier between metal electrodes, leading to increase of the interfacial contact resistance [12]. However, this shortage can be solved to a certain extent by using Ru as the supporting substrate, since the interaction between C and Ru atoms at graphene/Ru (0001) interface is of covalent nature, resulting in a large amount of tunneling pathways [12]. Also the strong adhesion between graphene and Ru substrate can largely avoid delamination upon external mechanical forces and will be helpful for potential applications like MEMS switches [21].

3 Conclusions

In this paper, the performance and failure mechanisms of microscale electrical contacts of metal/metal, metal/graphene systems were investigated by using conductive atomic force microscope (C-AFM). Based on contact mechanics calculation, a single-asperity contact experimental setup and conditions had been designed, which could well simulate the asperity-level contact condition in a MEMS switch (with similar contact pressure and current density).

The phenomenon of "intermittent failure" in single-asperity electrical contacts at metal/metal interfaces was observed. In the atmospheric environment, the current between the Ir-coated conductive tip and the Au-coated or Ru-coated substrate fluctuated sharply with the increase of contact cycles. X-ray photoelectron spectroscopy (XPS) and High-resolution tunneling electron microscopy (HRTEM) results demonstrated that carbonaceous contaminants adsorbed on the metal surface are the main cause of "intermittent failure".

Electrical contact between Ir-coated tip and single-layer graphene grown on Ru (0001) substrate showed much lower adhesion and stable contact resistance as compared to direct metal/metal contact. The adsorption of carbonaceous contaminants was reduced on graphene due to less chemical reactivity and lower surface energy of graphene than that of metal.

This work presents an experimental platform to simulate asperity-level contact condition in micro-electro-mechanical systems (MEMS) switch, and opens an avenue for design and fabrication of microscale electrical contact system.

Acknowledgements

The authors would like to acknowledge the support of the National Natural Science Foundation of China (Grant Nos. 11890671, 61774096, and 51935006), National Science and Technology Major Project (2017-VII-0013-0110), and the Fundamental Research Funds for the Central Universities.

References

[1] Bian W, Zhao J H, You Z. Low voltage, high speed and small area in-plane MEMS switch. *J Micromech Microeng* **29**(6): 065014 (2019)

[2] Streller F, Wabiszewski G E, Carpick R W. Next-generation nanoelectromechanical switch contact materials: a low-power mechanical alternative to fully electronic field-effect transistors. *IEEE Nanotechnol Mag* **9**(1): 18–24 (2015)

[3] Yang F, Yang J, Qi Y B, de Boer M P, Carpick R W, Rappe A M, Srolovitz D J. Mechanochemical effects of adsorbates at nanoelectromechanical switch contacts. *ACS Appl Mater Interfaces* **11**(42): 39238–39247 (2019)

[4] Lee J O, Song Y H, Kim M W, Kang M H, Oh J S, Yang H H, Yoon J B. A sub-1-volt nanoelectromechanical switching device. *Nat Nanotechnol* **8**(1): 36–40 (2013)

[5] Peschot A, Poulain C, Souchon F, Charvet P L, Bonifaci N, Lesaint O. Contact degradation due to material transfer in MEM switches. *Microelectron Reliab* **52**(9–10): 2261–2266 (2012)

[6] Brand V, Baker M S, de Boer M P. Impact of contact materials and operating conditions on stability of micromechanical switches. *Tribol Lett* **51**(3): 341–356 (2013)

[7] Liao M Z, Wu Z W, Du L J, Zhang T T, Wei Z, Zhu J Q, Yu H, Tang J, Gu L, Xing Y X, Yang R, Shi D X, Yao Y G, Zhang G Y. Twist angle-dependent conductivities across MoS_2/graphene heterojunctions. *Nat Commun* **9**: 4068(2018)

[8] Cao L M, Zhou G H, Wang Q Q, Ang L K, Ang Y S. Two-dimensional van der Waals electrical contact to monolayer $MoSi_2N_4$. *Appl Phys Lett* **118**(1): 013106 (2021)

[9] Li P, Jing G S, Zhang B, Sando S, Cui T H. Single-crystalline monolayer and multilayer graphene nano switches. *Appl Phys Lett* **104**(11): 113110 (2014)

[10] Koren E, Leven I, Lortscher E, Knoll A, Hod O, Duerig U. Coherent commensurate electronic states at the interface between misoriented graphene layers. *Nat Nanotechnol* **11**(9): 752–757 (2016)

[11] Chari T, Ribeiro-Palau R, Dean C R, Shepard K. Resistivity of rotated graphite-graphene contacts. *Nano Lett* **16**(7): 4477–4482 (2016)

[12] Song A S, Shi R Y, Lu H L, Gao L, Li Q Y, Guo H, Liu Y M, Zhang J, Ma Y, Tan X, et al. Modeling atomic-scale electrical contact quality across two-dimensional interfaces. *Nano Lett* **19**(6): 3654–3662 (2019)

[13] Yu Z W, Song A S, Sun L Z, Li Y L Z, Gao L, Peng H L, Ma T B, Liu Z F, Luo J B. Understanding interlayer contact conductance in twisted bilayer graphene. *Small* **16**(15): 1902844 (2020)

[14] Vishnubhotla S B, Chen R M, Khanal S R, Li J, Stach E A, Martini A, Jacobs T D B. Quantitative measurement of contact area and electron transport across platinum nanocontacts for scanning probe microscopy and electrical nanodevices. *Nanotechnology* **30**(4): 045705 (2019)

[15] Yu K M, Zou K, Lang H J, Peng Y T. Nanofriction characteristics of h-BN with electric field induced electrostatic interaction. *Friction* **9**(6): 1492–1503 (2021)

[16] Vazirisereshk M R, Sumaiya S A, Martini A, Baykara M Z. Measurement of electrical contact resistance at nanoscale gold-graphite interfaces. *Appl Phys Lett* **115**(9): 091602 (2019)

[17] Vazirisereshk M R, Sumaiya S A, Chen R M, Baykara M Z, Martini A. Time-dependent electrical contact resistance at the nanoscale. *Tribol Lett* **69**(2): 50 (2021)

[18] Simmons J G. Generalized formula for the electric tunnel effect between similar electrodes separated by a thin insulating film. *J Appl Phys* **34**(6): 1793–1803 (1963)

[19] Matthews N, Hagmann M J, Mayer A. Comment: "Generalized formula for the electric tunnel effect between similar electrodes separated by a thin insulating film". *J Appl Phys* **123**(13): 136101 (2018)

[20] Pan Y, Zhang H G, Shi D X, Sun J T, Du S X, Liu F, Gao H J. Highly ordered, millimeter-scale, continuous, single-crystalline graphene monolayer formed on Ru (0001). *Adv Mater* **21**(27): 2777–2780 (2009)

[21] Shi R Y, Gao L, Lu H L, Li Q Y, Ma T B, Guo H, Du S X, Feng X Q, Zhang S, Liu Y M, Cheng P, Hu Y Z, Gao H J, Luo J B. Moire superlattice-level stick-slip instability originated from geometrically corrugated graphene on a strongly interacting substrate. *2D Mater* **4**(2): 025079 (2017)

Tianbao MA. He received his bachelor degree in mechanical engineering from Northeastern University, Shenyang, China in 2003, and Ph.D. degree in mechanical engineering from Tsinghua University, Beijing, China in 2007. He is an associate professor and vice director of State Key Laboratory of Tribology, Tsinghua University. His research areas include fundamentals of friction, superlubricity, etc. He has authored more than 80 peer-reviewed journal articles in related fields.

Zhiwei YU. He received his bachelor degree in mechanical engineering from Tsinghua University, Beijing, China in 2016. Then he was a Ph.D. student in the State Key Laboratory of Tribology at the same university. He obtained his Ph.D. degree in mechanical engineering at Tsinghua University in 2021. Now he is a system on chip (SoC) development engineer of Inspur Beijing Electronic Information Industry Co., Ltd. His research interests include microelectromechanical systems and micro/nano electrical contacts.